

## **Boosting Electrocatalytic Water Oxidation of NiFe Layered Double Hydroxide *via* the Synergy of 3d-4f Electron Interaction and Citrate Intercalation**

*Shuo Chen,<sup>a</sup> Zhicheng Zheng,<sup>a</sup> Qing ying Li,<sup>a</sup> Hao Wan,<sup>b,\*</sup> Gen Chen,<sup>a</sup> Ning Zhang,<sup>a</sup> Xiaohe Liu,<sup>a,b,\*</sup> Renzhi Ma<sup>c,\*</sup>*

<sup>a</sup> School of Materials Science and Engineering, Central South University, Changsha, Hunan 410083, P. R. China. E-mail: liuxh@csu.edu.cn

<sup>b</sup> Zhongyuan Critical Metals Laboratory, Zhengzhou University, Zhengzhou 450001, P. R. China. E-mail: wanhao@zzu.edu.cn

<sup>c</sup> International Center for Materials Nanoarchitectonics (WPI-MANA), National Institute for Materials Science (NIMS), Namiki 1-1, Tsukuba, Ibaraki 305-0044, Japan. E-mail: Ma.Renzhi@nims.go.jp

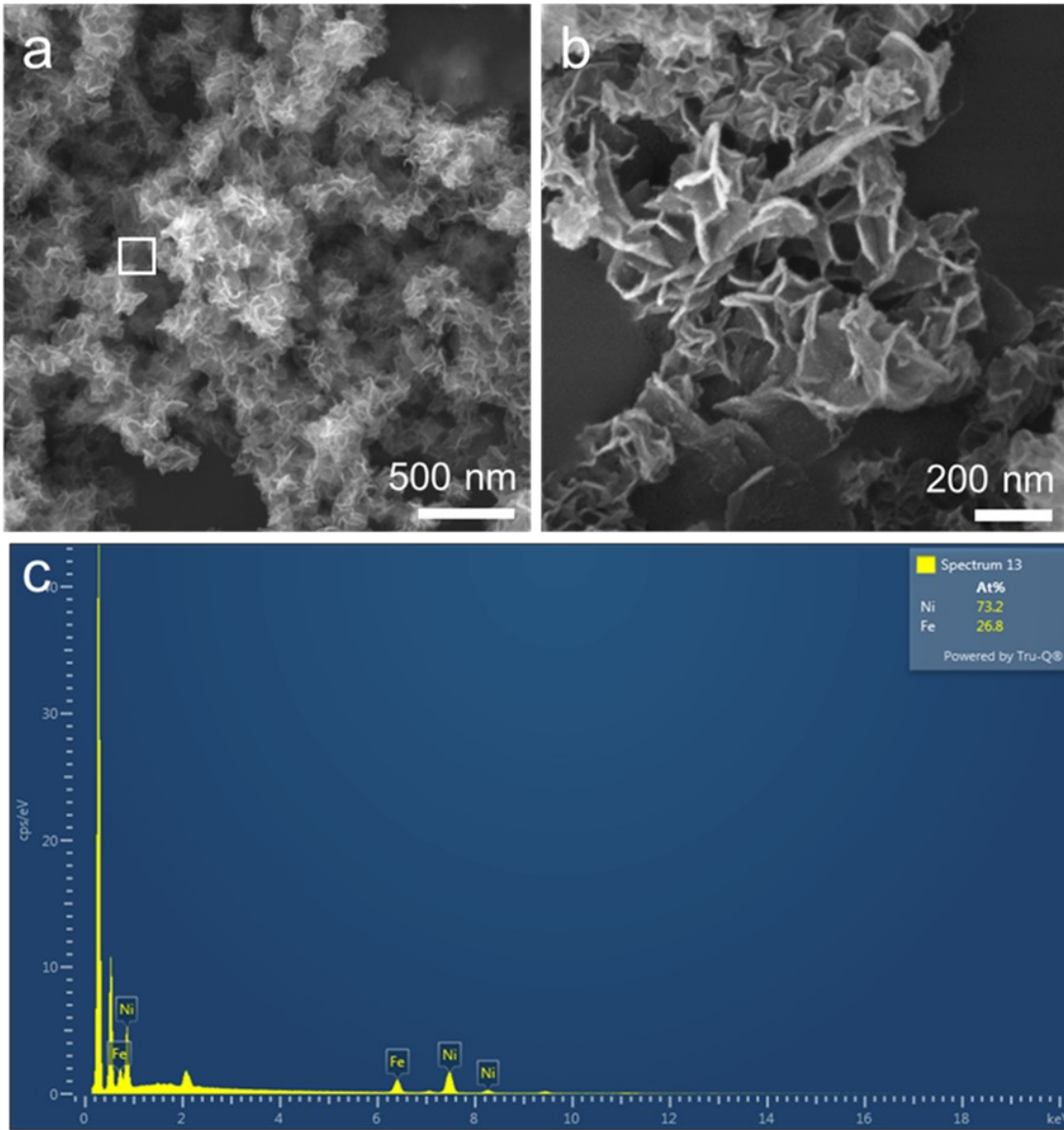


Figure S1. (a-b) SEM images and (c) EDX result of  $\text{Ni}_2\text{Fe}_1$  PNs.

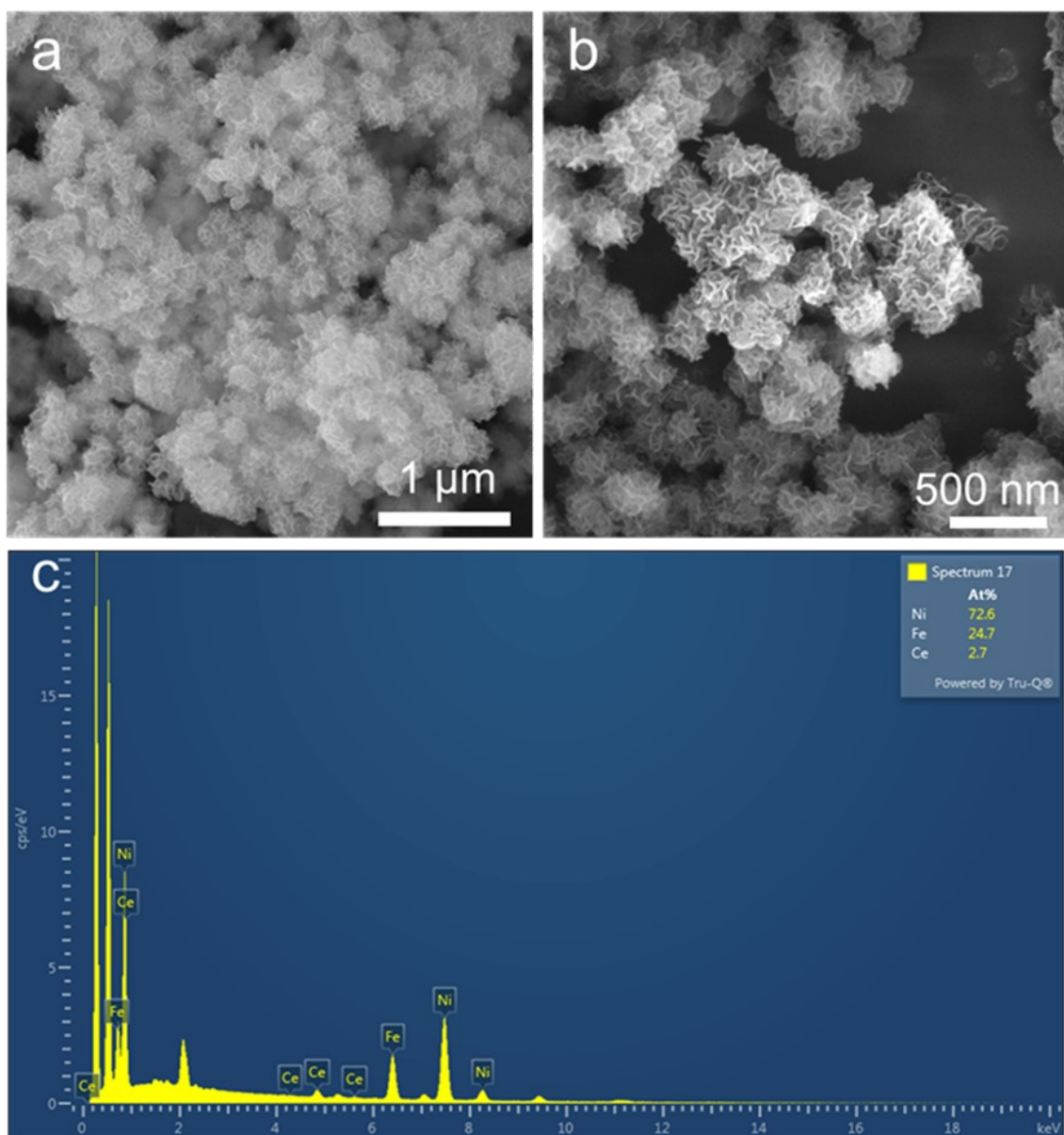


Figure S2. (a-b) SEM images and (c) EDX result of  $\text{Ni}_2\text{Fe}_{0.9}\text{Ce}_{0.1}$  PNs.

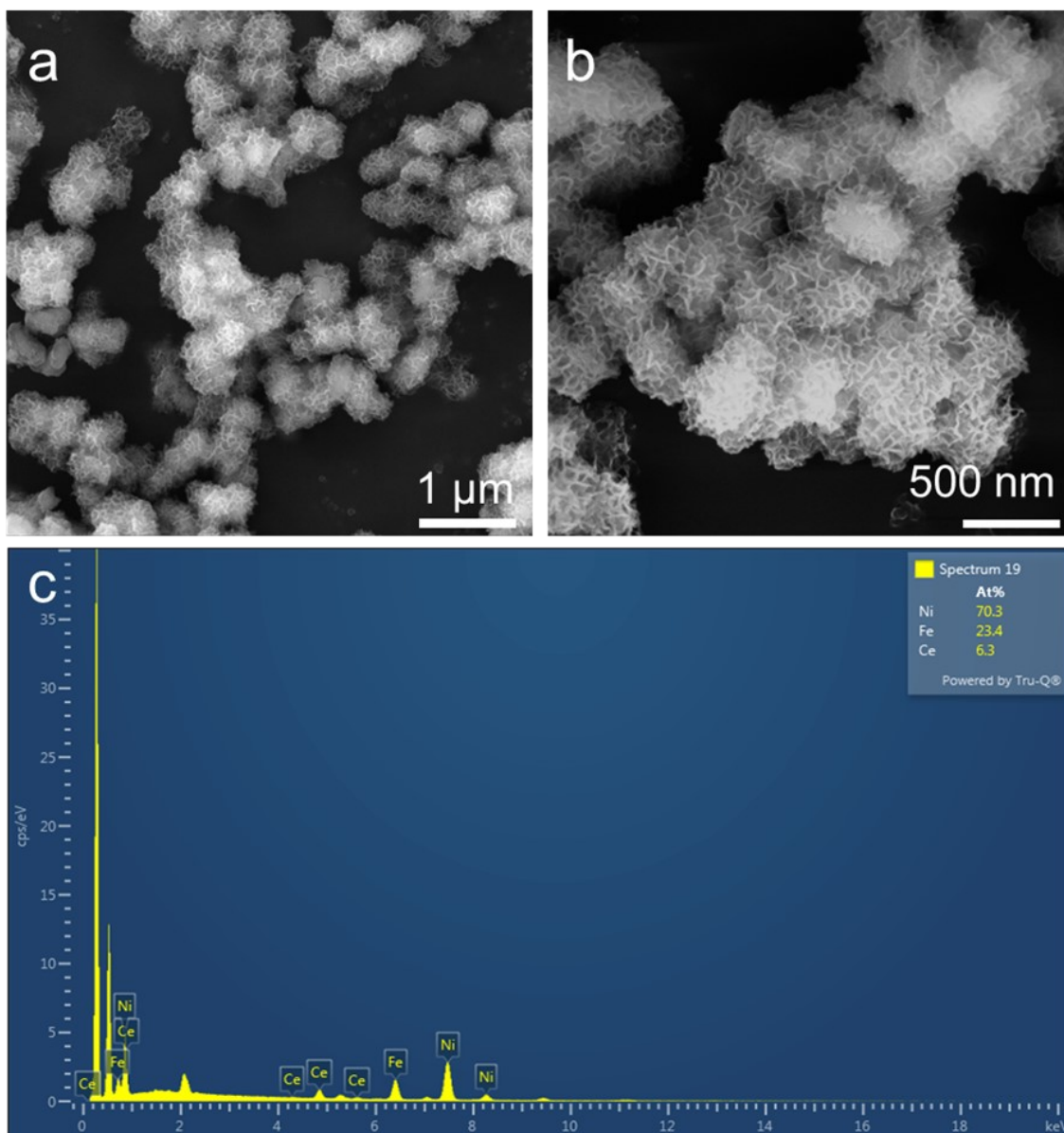


Figure S3. (a-b) SEM images and (c) EDX result of  $\text{Ni}_2\text{Fe}_{0.8}\text{Ce}_{0.2}$  PNs.

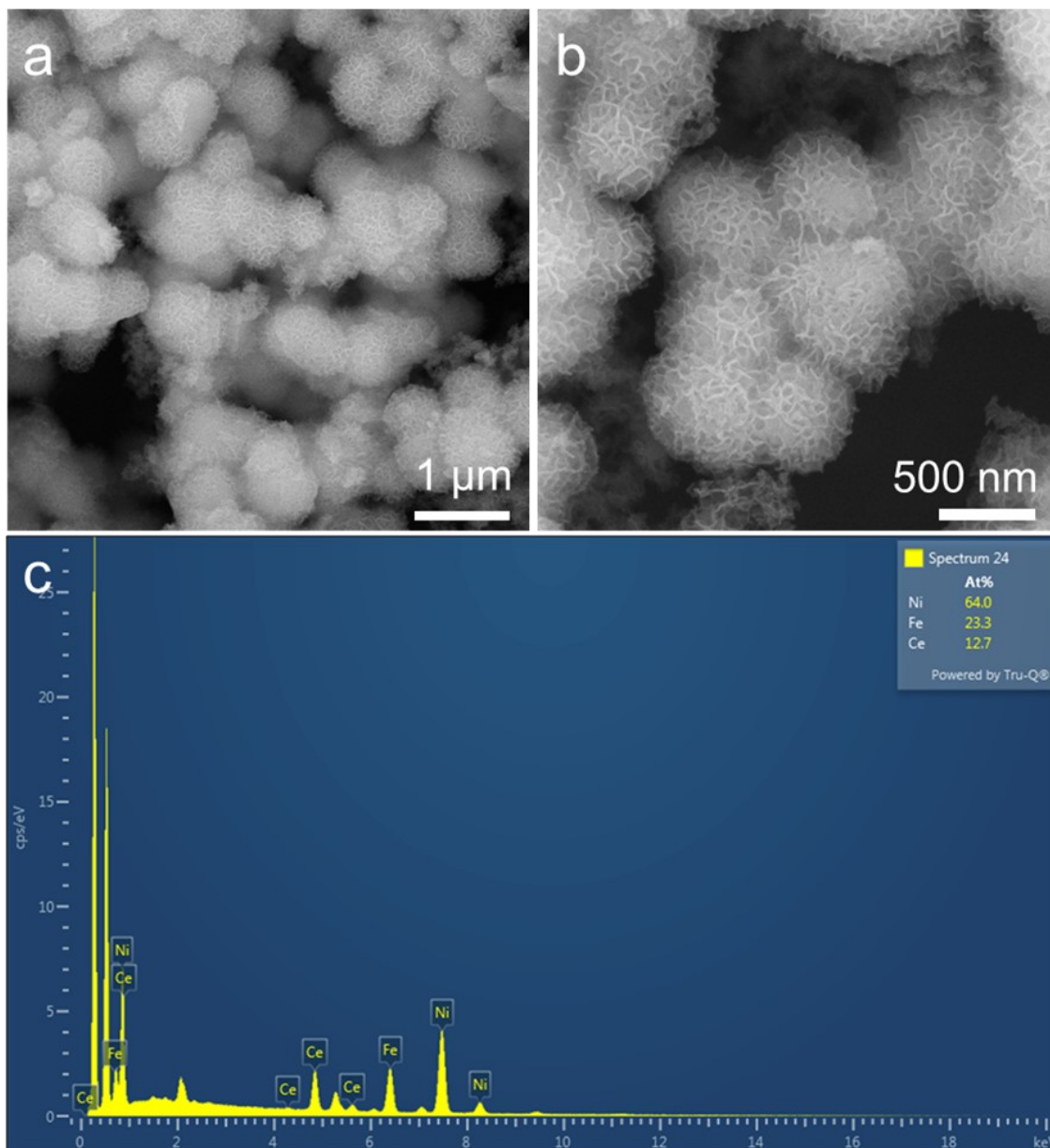


Figure S4. (a-b) SEM images and (c) EDX result of  $\text{Ni}_2\text{Fe}_{0.7}\text{Ce}_{0.3}$  PNs.

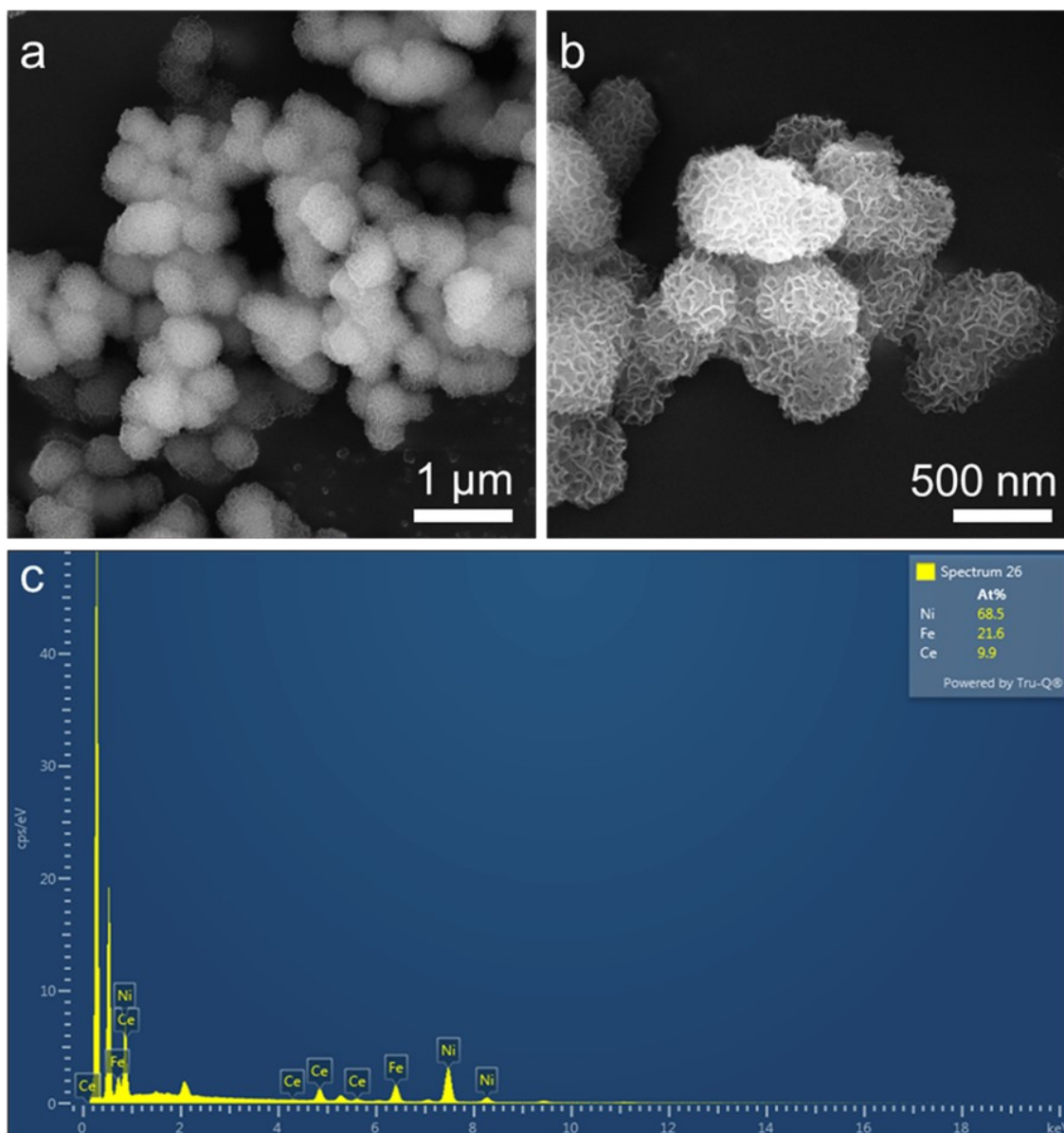


Figure S5. (a-b) SEM images and (c) EDX result of  $\text{Ni}_2\text{Fe}_{0.6}\text{Ce}_{0.4}$  PNs.



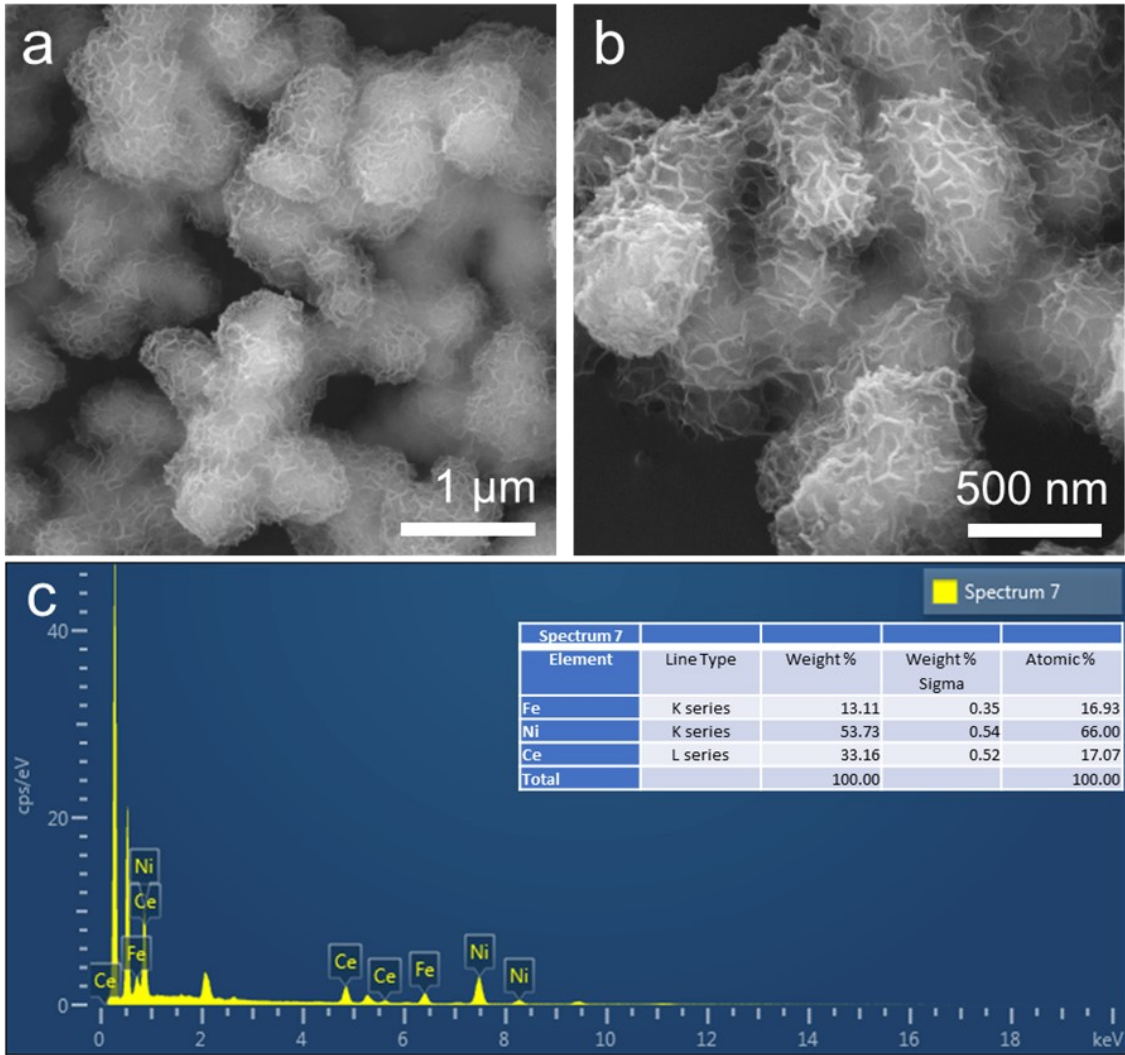


Figure S6. (a-b) SEM image and (c) EDX result of  $\text{Ni}_2\text{Fe}_{0.5}\text{Ce}_{0.5}$  PNs.

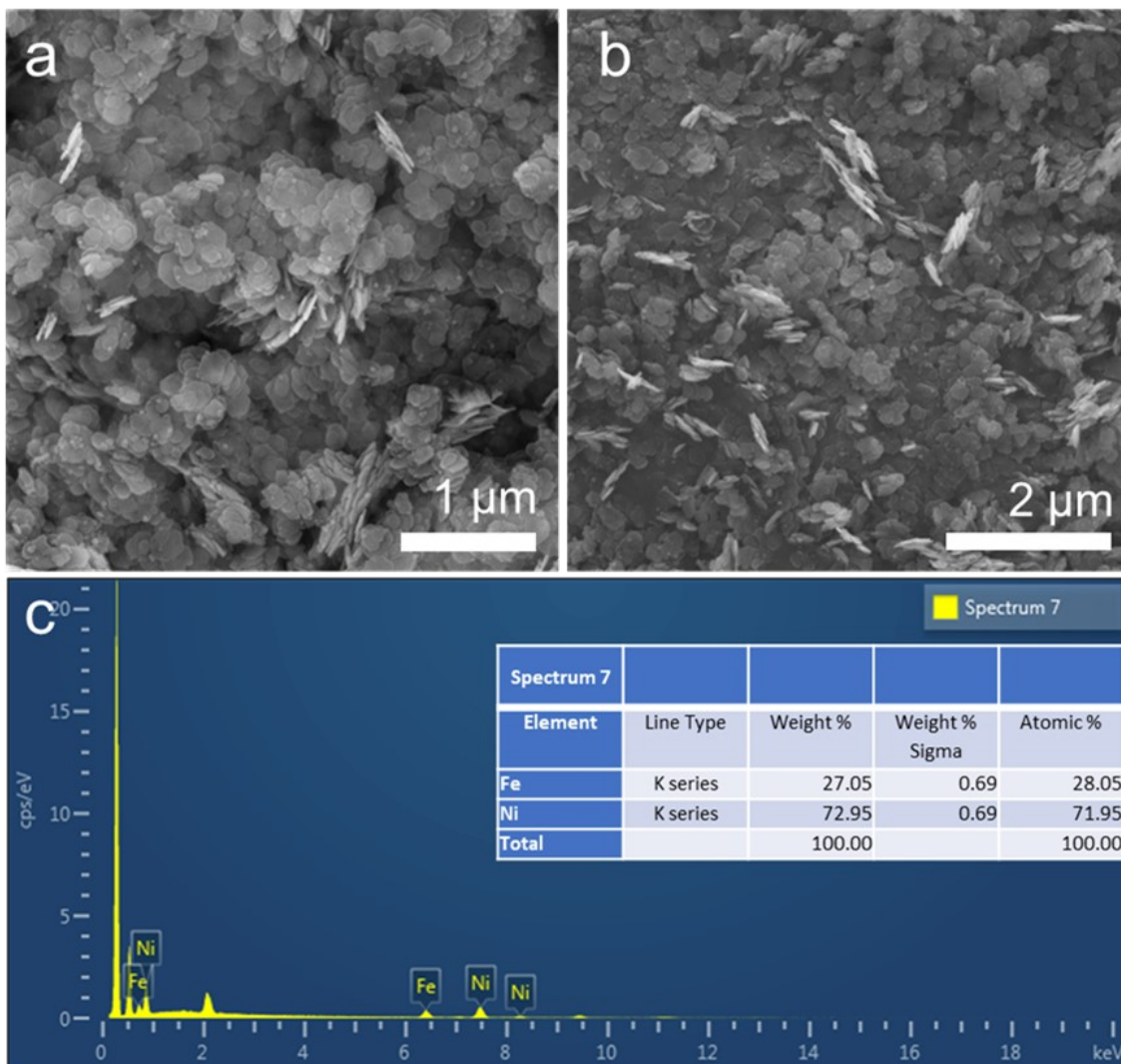


Figure S7. (a-b) SEM images and (c) EDX result of  $\text{Ni}_2\text{Fe}_1$  Ns.



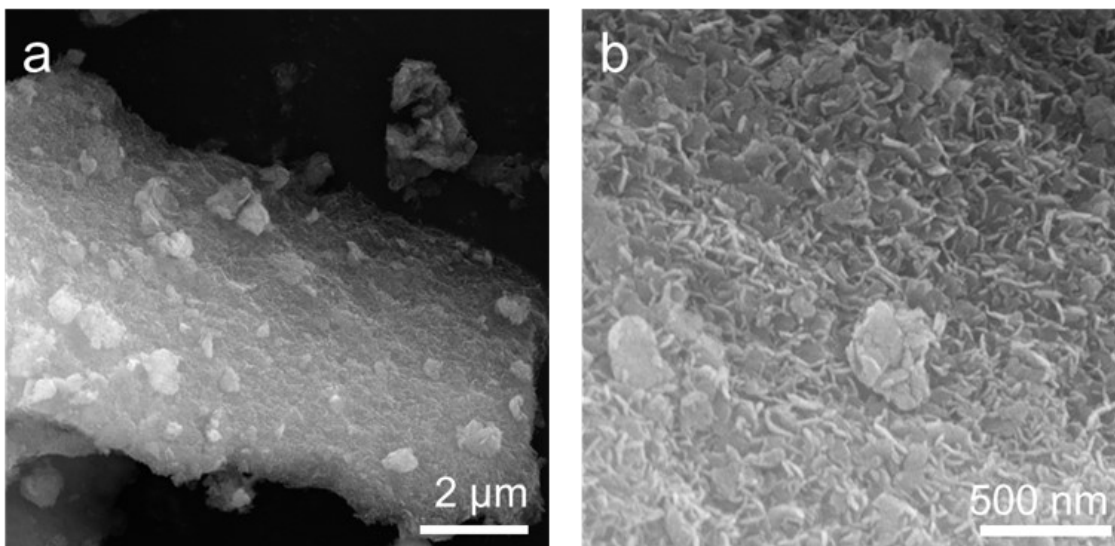


Figure S8. (a-b) SEM images of  $\text{Ni}_2\text{Fe}_1$  LDH product prepared without citrate additive.

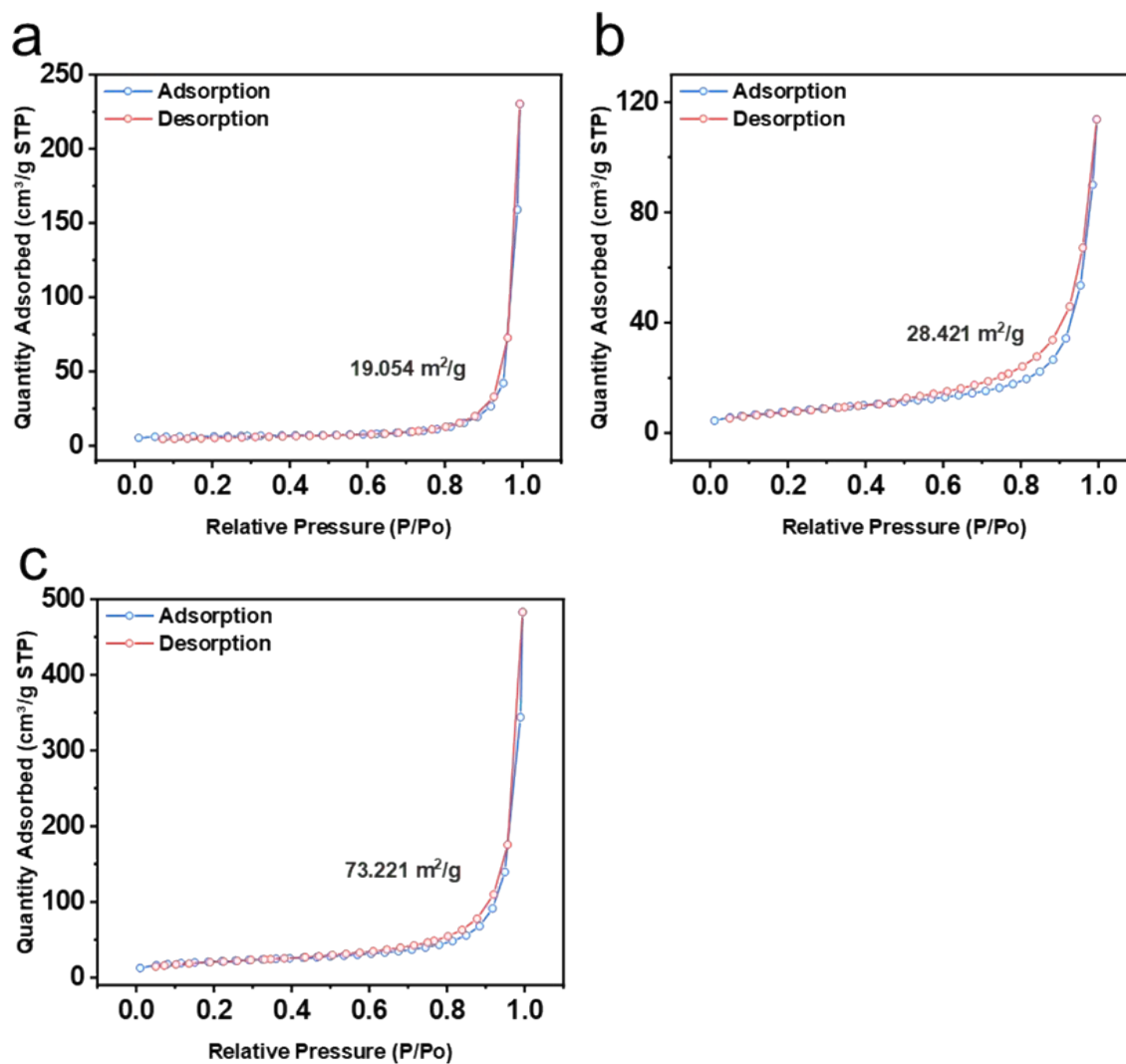


Figure S9.  $\text{N}_2$  sorption/desorption isotherms of (a)  $\text{Ni}_2\text{Fe}_1$  Ns, (b)  $\text{Ni}_2\text{Fe}_{0.7}\text{Ce}_{0.3}$  PN and (c)  $\text{Ni}_2\text{Fe}_1$  PN.

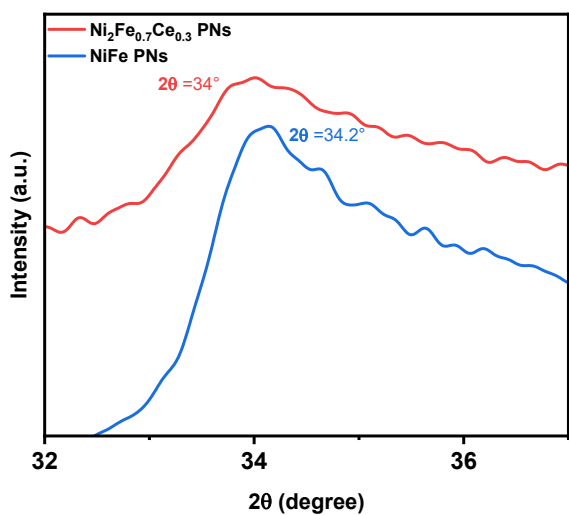


Figure S10. Magnified XRD pattern for (012) peak.

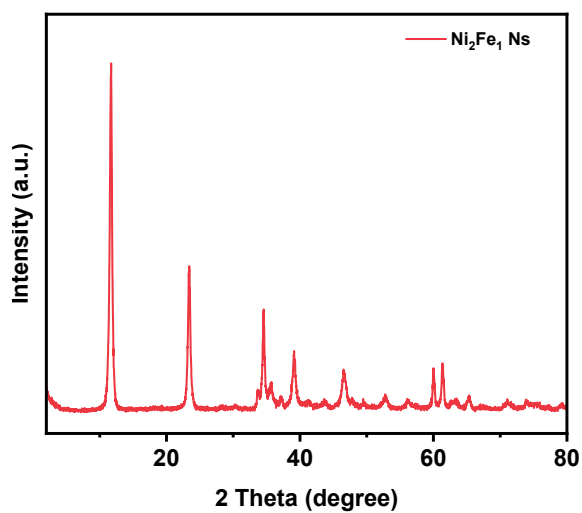


Figure S11. XRD patterns of  $\text{Ni}_2\text{Fe}_1$  Ns.

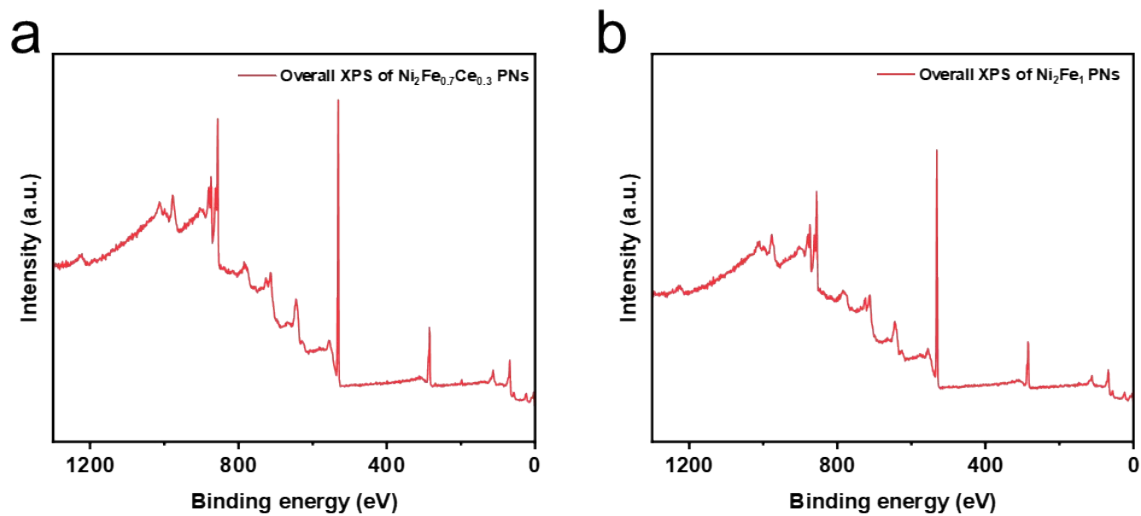


Figure S12. Overall XPS surveys of (a)  $\text{Ni}_2\text{Fe}_{0.7}\text{Ce}_{0.3}$  PNs and (b)  $\text{Ni}_2\text{Fe}_1$  PNs.

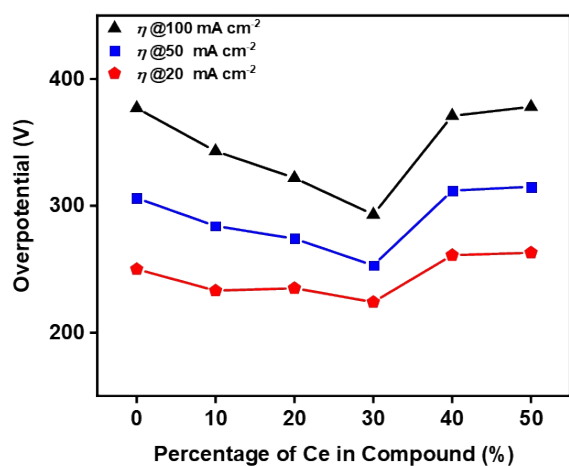


Figure S13. Overpotential at different current density.

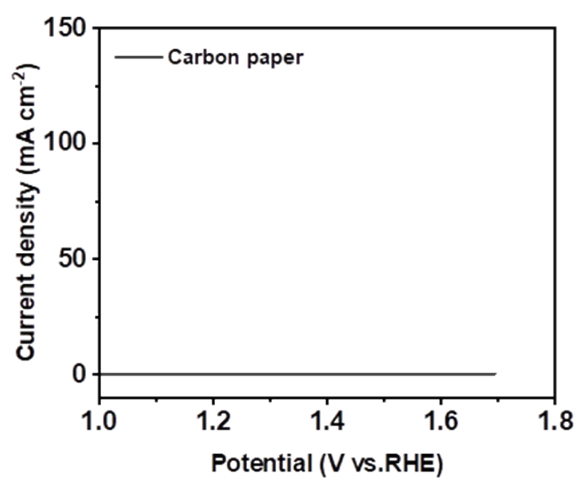


Figure S14. OER activity of carbon paper.

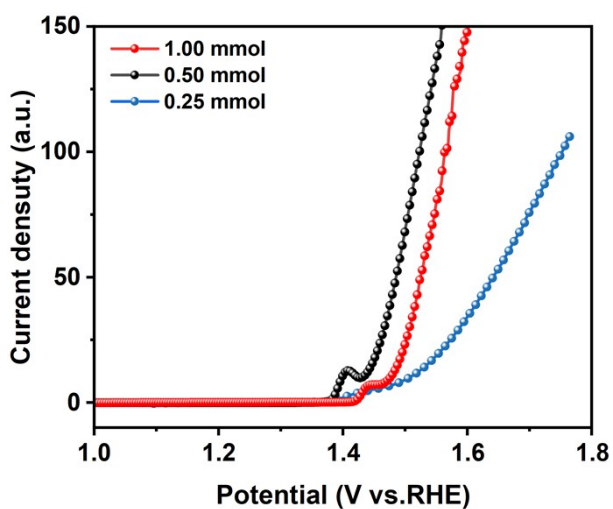


Figure S15. LSV curves of catalysts with different citrate additive amounts.

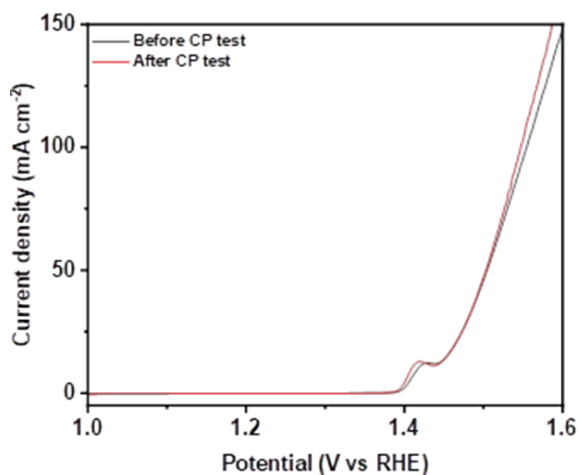


Figure S16. LSV curves of  $\text{Ni}_2\text{Fe}_{0.7}\text{Ce}_{0.3}$  PNs without iR-correction before and after Chronopotentiometric test.

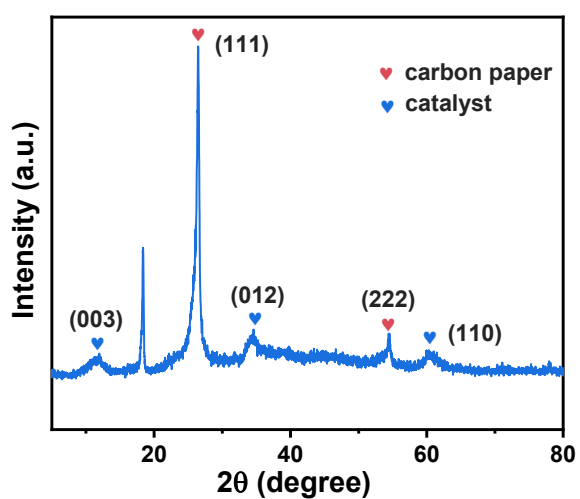


Figure S17. XRD pattern of  $\text{Ni}_2\text{Fe}_{0.7}\text{Ce}_{0.3}$  PNs after chronopotentiometric test.

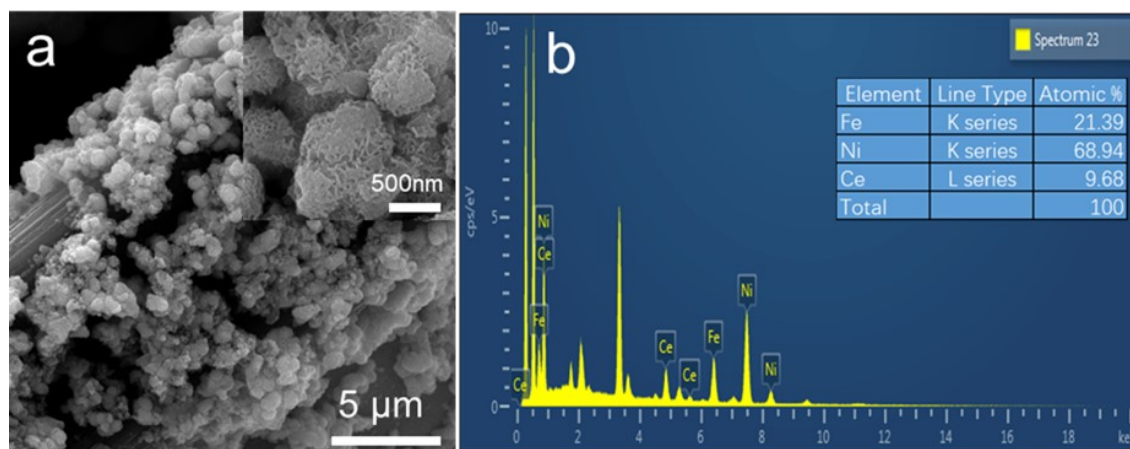


Figure S18. (a) SEM images and (b) EDX result after chronopotentiometric test.

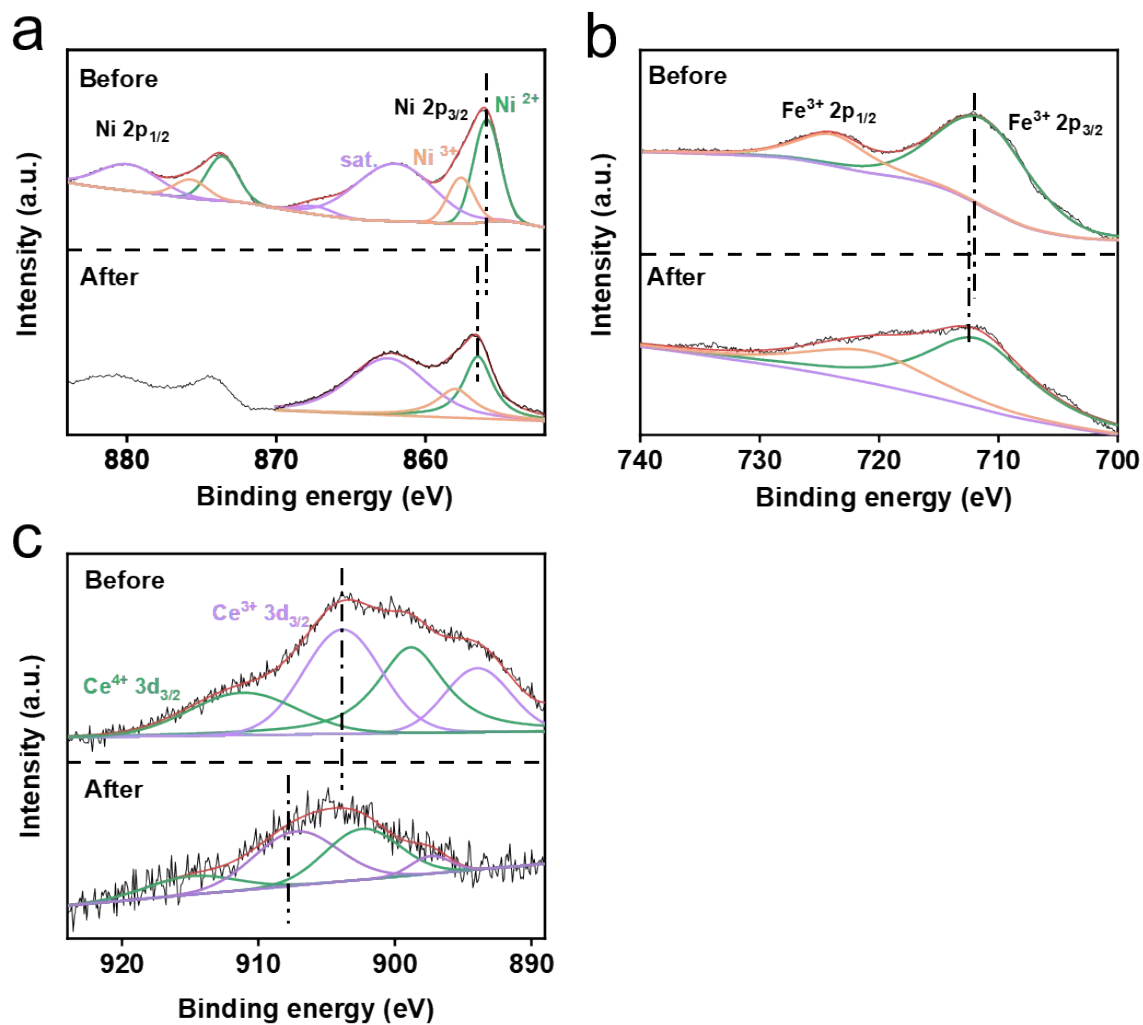


Figure S19. XPS spectra after the chronopotentiometric test. (a) Ni 2p, (b) Fe 2p and (c) Ce 3d.

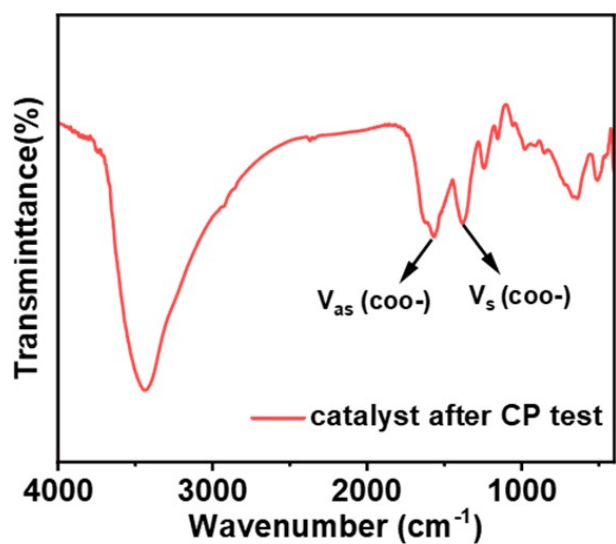


Figure S20. The FT-IR spectrum of Ni<sub>2</sub>Fe<sub>0.7</sub>Ce<sub>0.3</sub> PN after the chronopotentiometric test.

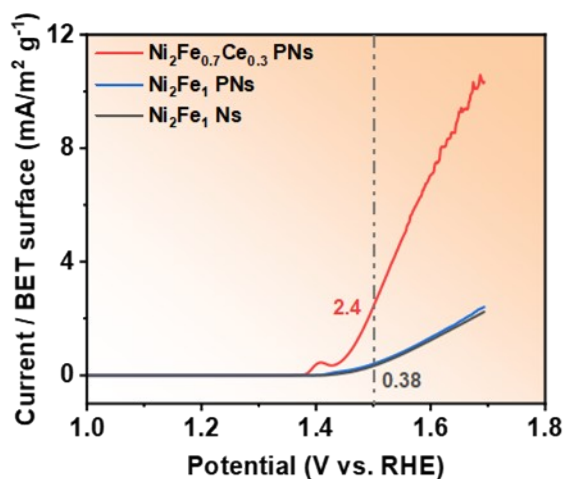


Figure S21. LSV curves normalized by BET surface areas.

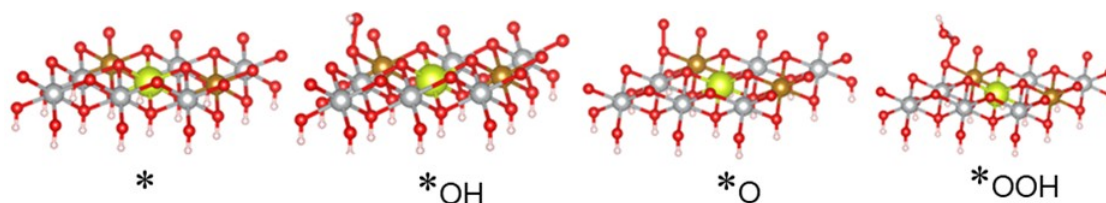


Figure S22. Adsorption models of each OER elementary step.

Table S1. Binding energies and corresponding fitting relative areas in XPS spectra

Orbits	Ni <sub>2</sub> Fe <sub>0.7</sub> Ce <sub>0.3</sub> PNs	Ni <sub>2</sub> Fe <sub>1</sub> PNs
Fe <sup>3+</sup> 2p <sub>3/2</sub>	711.43 eV / 311657.4	712.50 eV / 338187.2
Fe <sup>3+</sup> 2p <sub>1/2</sub>	724.09 eV / 155828.7	724.91 eV / 169093.6
Ni <sup>2+</sup> 2p <sub>3/2</sub>	856.07 eV / 214567.7	855.69 eV / 237217.3
Ni <sup>3+</sup> 2p <sub>1/2</sub>	857.63 eV / 96498.85	857.21 eV / 83106.64
Ce <sup>3+</sup> 3d <sub>3/2</sub>	904.33 eV / 57828.39	/
Ce <sup>4+</sup> 3d <sub>3/2</sub>	910.83 eV / 70843.83	/



Table S2. Overpotential delivering different current densities

	<b>20mA cm<sup>-2</sup></b>	<b>50mA cm<sup>-2</sup></b>	<b>100mA cm<sup>-2</sup></b>
Ni <sub>2</sub> Fe <sub>1</sub> PNs	250	306	377
Ni <sub>2</sub> Fe <sub>0.9</sub> Ce <sub>0.1</sub>	233	284	343
Ni <sub>2</sub> Fe <sub>0.8</sub> Ce <sub>0.2</sub>	235	274	322
Ni <sub>2</sub> Fe <sub>0.7</sub> Ce <sub>0.3</sub>	224	253	293
Ni <sub>2</sub> Fe <sub>0.6</sub> Ce <sub>0.4</sub>	261	312	371
Ni <sub>2</sub> Fe <sub>0.5</sub> Ce <sub>0.5</sub>	263	315	378
Ni <sub>2</sub> Fe <sub>1</sub> Ns	352	419	534
RuO <sub>2</sub>	381		

Table S3. The values of parameters in the fitting circuit

	<b>Ni<sub>2</sub>Fe<sub>0.5</sub>Ce<sub>0.5</sub></b>	<b>Ni<sub>2</sub>Fe<sub>0.6</sub>Ce<sub>0.4</sub></b>	<b>Ni<sub>2</sub>Fe<sub>0.7</sub>Ce<sub>0.3</sub></b>	<b>Ni<sub>2</sub>Fe<sub>0.8</sub>Ce<sub>0.2</sub></b>	<b>Ni<sub>2</sub>Fe<sub>0.5</sub>Ce<sub>0.5</sub></b>	<b>Ni<sub>2</sub>Fe<sub>1</sub> PNs</b>	<b>Ni<sub>2</sub>Fe<sub>1</sub> Ns</b>
	<b>PNs</b>	<b>PNs</b>	<b>PNs</b>	<b>PNs</b>	<b>PNs</b>		
R <sub>s</sub> (Ω)	3.161	2.941	2.915	2.877	2.863	2.783	2.821
CPE-1-T	0.0049445	0.011861	0.01443	0.015921	0.0065464	0.00025401	0.0020007
CPE-1-P	0.60365	0.54977	0.76804	0.81399	0.67977	0.87632	0.71344
R <sub>ct1</sub> (Ω)	1.096	1.187	0.28386	0.24508	0.52489	0.64906	2.167
CPE-2-T	0.054842	0.041936	0.070164	0.06374	0.064373	0.051382	0.0078659
CPE-2-T	0.7567	0.78909	0.86533	0.85811	0.79748	0.65801	0.7131
R <sub>ct2</sub> (Ω)	9.384	7.162	4.232	4.563	4.379	5.229	20.98

Table S4. OER activity of recently reported NiFe-based catalysts

Catalysts	Overpotential at 20 mA cm <sup>-2</sup>	Supporter	Loading Capacity (mg cm <sup>-1</sup> )	References
Ni <sub>2</sub> Fe <sub>0.7</sub> Ce <sub>0.3</sub> PNs	224	CP	0.4	This work
NiFeS@Ti <sub>3</sub> C <sub>2</sub> MXene/NF	290	NF	1.25	1
CoO@NiFe LDH/NF	225	NF	0.78	2
Co <sub>1.98</sub> -NiFe LDH	236	CP	1	3
Fe <sub>2</sub> P-NiCoP	239	NF		4
NiFe LDH-Ci/CC	240	CC	0.67	5
Ni-Fe LDH DSNCs	246	CP	0.22	6
NiFeW- LDH@CP	248	CP	0.8	7
NiFe <sub>2</sub> O <sub>4</sub> @N/rGO	252	NF	1	8
NiFe-Pi/P	255	NF	2	9
(Ni <sub>0.5</sub> Fe <sub>0.5</sub> )C <sub>2</sub> O <sub>4</sub> nanorods	266	NF		10
NiFe PBAs	267	rotating disk electrode (RDE)	0.15	11
CNT@NiFe-LDH NS	270	NF	0.5	12
MoNiFe-LDH	317	glass carbon		13

CP, CC, NF refer to carbon paper, carbon cloth and nickel foam respectively.

## References

1. D. Chanda, K. Kannan, J. Gautam, M. M. Meshesha, S. G. Jang, V. A. Dinh and B. L. Yang, *Appl. Catal., B*, 2023, **321**.
2. Z. Wang, J. Zhang, Q. Yu, H. Yang, X. Chen, X. Yuan, K. Huang and X. Xiong, *Chem. Eng. J.*, 2021, **410**.
3. Y. Yang, S. Wei, Y. Li, D. Guo, H. Liu and L. Liu, *Appl. Catal., B*, 2022, **314**.
4. M. Xiao, C. Zhang, P. Wang, W. Zeng, J. Zhu, Y. Li, W. Peng, Q. Liu, H. Xu, Y. Zhao, H. Li, L. Chen, J. Yu and S. Mu, *Materials Today Physics*, 2022, **24**.
5. Z. Wang, J. Zhang, Q. Wang, X. Jiang, K. Huang and X. Xiong, *Journal of Materials Science*, 2021, **56**, 8115-8126.
6. J. Zhang, L. Yu, Y. Chen, X. F. Lu, S. Gao and X. W. D. Lou, *Adv Mater*, 2020, **32**, e1906432.
7. P.-F. Guo, Y. Yang, W.-J. Wang, B. Zhu, W.-T. Wang, Z.-Y. Wang, J.-L. Wang, K. Wang, Z.-H. He and Z.-T. Liu, *Chem. Eng. J.*, 2021, **426**.

8. L. Cao, Z. Li, K. Su, M. Zhang and B. Cheng, *Journal of Energy Chemistry*, 2021, **54**, 595-603.
9. W. Li, M. Chen, Y. Lu, P. Qi, G. Liu, Y. Zhao, H. Wu and Y. Tang, *Applied Surface Science*, 2022, **598**.
10. H. Hu, X. Lei, S. Li, R. Peng and J. Wang, *New Journal of Chemistry*, 2022, **46**, 328-333.
11. M. Jiang, X. Fan, S. Cao, Z. Wang, Z. Yang and W. Zhang, *Journal of Materials Chemistry A*, 2021, **9**, 12734-12745.
12. H. Chen, P. Zhang, R. Xie, Y. Xiong, C. Jia, Y. Fu, P. Song, L. Chen, Y. Zhang and T. Liao, *Advanced Materials Interfaces*, 2021, **8**.
13. Z. Yin, X. Liu, M. Cui, Z. Cao, A. Liu, L. Gao, T. Ma, S. Chen and Y. Li, *Materials Today Sustainability*, 2022, **17**.